Photon Subtraction by Many-Body Decoherence

C. R. Murray,[1] I. Mirgorodskiy,[2] C. Tresp,[3] C. Braun,[3] A. Paris-Mandoki,[3]
A. V. Gorshkov,[4] S. Hofferberth,[3] and T. Pohl[1]

[1]*Center for Quantum Optics and Quantum Matter, Department of Physics and Astronomy,
Aarhus University, Ny Munkegade 120, DK 8000 Aarhus C, Denmark*
[2]*5. Physikalisches Institut and Center for Integrated Quantum Science and Technology,
Universität Stuttgart, Pfaffenwaldring 57, 70569 Stuttgart, Germany*
[3]*Department of Physics, Chemistry and Pharmacy, University of Southern Denmark,
Campusvej 55, 5230 Odense-M, Denmark*
[4]*Joint Quantum Institute and Joint Center for Quantum Information and Computer Science,
NIST/University of Maryland, College Park, Maryland 20742, USA*

We experimentally and theoretically investigate the scattering of a photonic quantum field from another stored in a strongly interacting atomic Rydberg ensemble. Considering the many-body limit of this problem, we derive an exact solution to the scattering-induced spatial decoherence of multiple stored photons, allowing for a rigorous understanding of the underlying dissipative quantum dynamics. Combined with our experiments, this analysis reveals a correlated coherence-protection process in which the scattering from one excitation can shield all others from spatial decoherence. We discuss how this effect can be used to manipulate light at the quantum level, providing a robust mechanism for single-photon subtraction, and experimentally demonstrate this capability.

Dissipation in quantum many-body systems can provide a powerful resource for realizing and harnessing a wide variety of complex emergent phenomena [1]. This notion has since enabled new concepts and strategies in dissipative quantum computation [2], simulation [3], and many-body physics [4,5]. Quantum optics systems present natural settings for such physics since they are intrinsically driven and dissipative in nature. Here, the interplay between coherent driving, photon propagation, and dissipation can give rise to a broad range of nonequilibrium phenomena [6,7]. In combination with strong optical nonlinearities at the quantum level [8–24], this is now opening up a new frontier in strongly correlated nonequilibrium physics with photons [25–29]. In this direction, electromagnetically induced transparency (EIT) [30] in atomic Rydberg ensembles [31] has emerged as one of the most promising approaches [32–35] for achieving strong, and often dissipative, photon-photon interactions.

The nonlinearity in such systems arises from the Rydberg blockade [36] that prevents EIT for nearby photons, yielding strong nonlinear dispersion [23] or dissipation [22,37]. This mechanism has been successfully employed for few-body applications, such as all-optical switches [38–41] and two-photon phase gates [42], where in both cases an initially stored gate photon controls the state of a subsequently passing source photon. On the other hand, a deeper understanding of many-body dynamics in these systems still presents an outstanding and formidable challenge to both

theory and experiment. While the formation of three-body photon bound states has been studied [43] and reported [44] very recently, the observational signatures for the transition to many-body behavior have remained elusive.

In this work, we undertake such an extension of previous two-body applications [38–41] to multiple gate and source photons. Our experiments performed in this many-body regime indeed reveal clear deviations from previous theories [45,46] for single gate-photon states. Remarkably, it is possible to derive a closed solution of the general many-body problem that accounts for the interplay of coherent photon propagation, strong atom-atom interactions, and dissipative processes in an exact fashion. The new theory provides an excellent description of our experiments and reveals a correlated decoherence protection mechanism, where source photon scattering off one gate excitation shields all others behind it from spatial decoherence. Studying this backaction on the stored excitations, we show how it can be exploited to subtract a single photon from the retrieved gate field, and provide an experimental demonstration of this capability. In this way, the role of the source and gate fields are reversed, where the source field is now used to manipulate the stored gate field.

The basic idea and setup are illustrated in Figs. 1(a)–1(c). Initially, a multiphoton gate field is stored [47–49] as a collective spin wave in the Rydberg state $|c\rangle$ of an atomic ensemble to yield a system of n_g stored excitations. This is achieved via Rydberg EIT with a properly timed gate-photon
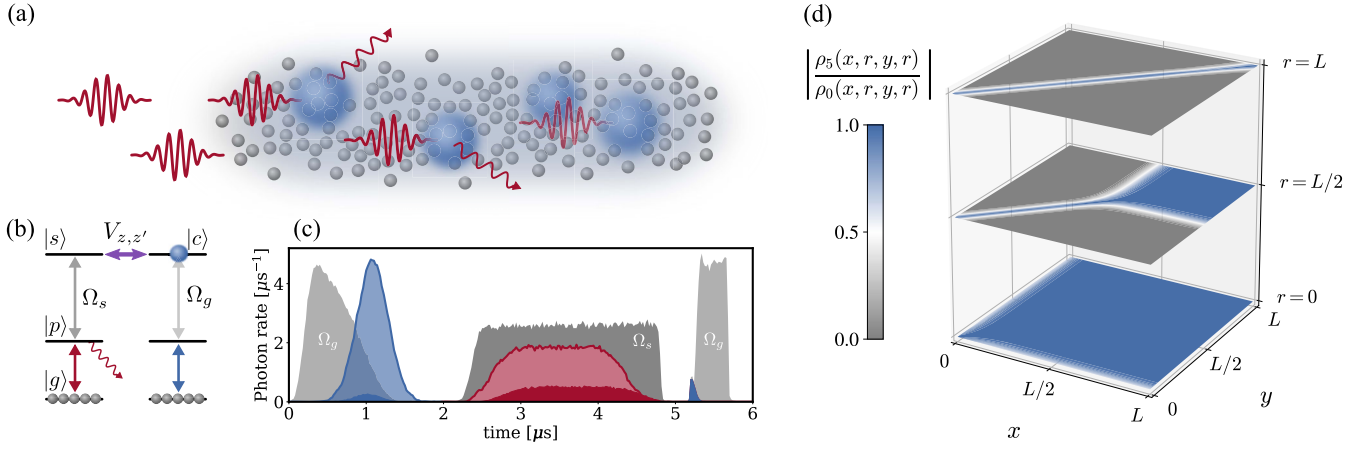
FIG. 1. (a) Schematics of the basic setting in which Rydberg spin wave excitations (blue) stored in an ultracold gas interact with secondary Rydberg polaritons formed by propagating photons (red), whose interaction-induced scattering causes decoherence of the stored spin waves. The underlying level scheme through which the initial gate (blue) and secondary source (red) photons are coupled to their respective Rydberg states $|c\rangle$ and $|s\rangle$ is shown in panel (b). Panel (c) shows the experimental pulse sequence for a complete cycle of storage, interaction, and retrieval stages. The blue and red curves show the gate and source field envelopes, respectively, where the light and dark traces indicate the incident and transmitted intensities. The gray curves show the control field envelopes (not to scale). Panel (d) shows the density matrix $\rho_5(x, r, y, r)$ of two stored gate excitations after scattering 5 source photons and illustrates the correlated nature of the associated decoherence process.

pulse and control field with Rabi frequency Ω_g as shown in Fig. 1(c). Subsequently, a second source field containing n_s photons is sent through the medium under EIT conditions with a different Rydberg state $|s\rangle$. The strong van der Waals interaction between $|s\rangle$ and $|c\rangle$ results in a spatially dependant level shift $V_{z,z'} = C_6/|z - z'|^6$ of $|s\rangle$, where z and z' are the positions of $|s\rangle$ and $|c\rangle$, respectively. This exposes the propagating source photons to a dissipative two-level medium of extent $2z_b$ surrounding each gate excitation. Here z_b denotes the blockade radius [50] within which the formation of a dark state polariton is blocked. The effective optical depth of this exposed medium is $\sim 4d_b$, where $2d_b$ is the optical depth per blockade radius. For large values of d_b, nearly all incoming source photons are scattered in the blockade region such that this setup can function as an efficient optical switch [38–41].

This scattering, however, does not leave the gate photons unaffected. Each source photon scattered off a blockade sphere carries information about the position of the Rydberg excitation that is causing the blockade [46]. The associated coherence loss from such projective spatial measurements typically leads to strong localization of the original spin wave state, thereby inhibiting its subsequent retrieval.

Formulating the described system in second quantization, we introduce the bosonic operator $\hat{\mathcal{E}}^\dagger(z, t)$ for the creation of a source photon at position z and time t, and similarly $\hat{P}^\dagger(z, t)$, $\hat{S}^\dagger(z, t)$, and $\hat{C}^\dagger(z, t)$ for the creation of collective atomic excitations in the states $|p\rangle$, $|s\rangle$, and $|c\rangle$, respectively [see Fig. 1(b)]. To describe the many-body decoherence dynamics of the stored excitations, we define the operator $\hat{\rho}(\vec{x}_{n_g}, \vec{y}_{n_g}, t) = \prod_{i=1}^{n_g} \hat{C}^\dagger(x_i, t) \prod_{i=1}^{n_g} \hat{C}(y_i, t)$, which characterizes the spatial coherence between different

configurations $\vec{x}_{n_g} \equiv x_1, x_2, \ldots, x_{n_g}$ and $\vec{y}_{n_g} \equiv y_1, y_2, \ldots, y_{n_g}$ of the stored excitations. The dynamics of this operator is governed by the following equation of motion,

$$\partial_t \hat{\rho}(\vec{x}_{n_g}, \vec{y}_{n_g}, t) = i \int_0^L dz \left(\sum_k V_{z,x_k} - \sum_k V_{z,y_k} \right)$$
$$\times \hat{S}^\dagger(z, t) \hat{\rho}(\vec{x}_{n_g}, \vec{y}_{n_g}, t) \hat{S}(z, t). \quad (1)$$

Here, we assume low-intensity source and gate fields and neglect the source-source and gate-gate interactions. To calculate the spin wave decoherence predicted by Eq. (1), we start from the initial system state $|\Psi_{n_g,n_s}\rangle$ of n_g stored gate excitations and n_s incident source photons. The elements of the stored spin wave density matrix can then be defined according to $\rho_{n_s}(\vec{x}_{n_g}, \vec{y}_{n_g}, t) = \langle \Psi_{n_g,n_s} | \hat{\rho}(\vec{x}_{n_g}, \vec{y}_{n_g}, t) | \Psi_{n_g,n_s} \rangle$. Solving the dynamics of $\rho_{n_s}(\vec{x}_{n_g}, \vec{y}_{n_g}, t)$ according to Eq. (1) to zeroth order in the source field bandwidth, the final state of the stored gate excitations $\rho_{n_s}(\vec{x}_{n_g}, \vec{y}_{n_g}) = \rho_{n_s}(\vec{x}_{n_g}, \vec{y}_{n_g}, t \to \infty)$ after the passage of all source photons can be calculated as

$$\rho_{n_s}(\vec{x}_{n_g}, \vec{y}_{n_g}) = [\Phi_{n_g}(\vec{x}_{n_g}, \vec{y}_{n_g})]^{n_s} \rho_0(\vec{x}_{n_g}, \vec{y}_{n_g}), \quad (2)$$

where $\rho_0(\vec{x}_{n_g}, \vec{y}_{n_g})$ is the initial state, and the quantity $\Phi_{n_g}(\vec{x}_{n_g}, \vec{y}_{n_g})$ is given by

$$\Phi_{n_g}(\vec{x}_{n_g}, \vec{y}_{n_g})$$
$$= 1 + \frac{d_b}{z_b} \int_0^L dz \frac{\sum_k V_{z,x_k} - \sum_k V_{z,y_k}}{(i + \sum_k V_{z,x_k})(i - \sum_k V_{z,y_k})}$$
$$\times \exp\left(\frac{d_b}{z_b} \int_0^z dz' \left[\frac{\sum_k V_{z',y_k}}{i - \sum_k V_{z',y_k}} - \frac{\sum_k V_{z',x_k}}{i + \sum_k V_{z',x_k}} \right] \right), \quad (3)$$

where $\mathcal{V}_{z,z'} = \gamma V_{z,z'}/\Omega^2$ is the rescaled interaction potential, and γ is the decay rate of $|p\rangle$. A detailed derivation of this expression is presented in Ref. [51].

The emergence of correlated decoherence can be readily understood by considering a dilute system of gate excitations, where the contribution from spatial configurations with overlapping blockade radii can be neglected. Initially, the incoming source photons interact with the first gate excitation located closest to the incident medium boundary. As described above, the associated projective measurement of its position drastically degrades its retrieval. However, in the strong scattering limit, it also causes near complete extinction of the source field such that all subsequent gate excitations are shielded from photon scattering, leaving their spatial coherence unaffected.

To reveal this effect from our solution, Eq. (2), consider the simplest situation of two gate excitations, now stored in the same spatial mode. The quantity $\rho_{n_s}(x, r, y, r)$ in this case characterizes how the local density component of one gate excitation, at a position r, affects the spatial coherence between x and y of the other excitation. In Fig. 1(d), we plot $\rho_{n_s}(x, r, y, r)$ for various values of r. Indeed, one finds that source photon scattering leads to almost complete decoherence, rendering $\rho_{n_s}(x, r, y, r)$ largely diagonal for $x, y < r$. For $x, y > r$, on the other hand, the coherence of one gate excitation with respect to x and y is preserved by scattering from the other excitation at position r.

We can gain further insight into the decoherence dynamics for multiple gate excitations in the limit of $d_b \gg 1$. In this case, the quantity $\Phi_{n_g}(\vec{x}_{n_g}, \vec{y}_{n_g})$ characterizing the final density matrix in Eq. (2) reduces to [51]

$$\Phi_{n_g}(\vec{x}_{n_g}, \vec{y}_{n_g}) \overset{d_b \to \infty}{\approx} \Phi_1(x_{\min}, y_{\min}), \qquad (4)$$

where $x_{\min} = \min\{\vec{x}_{n_g}\}$ and $y_{\min} = \min\{\vec{y}_{n_g}\}$ are the coherence coordinates of the first excitation. This result indeed shows that only the first excitation participates in the scattering dynamics. Since $\Phi_1(x_{\min}, y_{\min} \neq x_{\min}) = 0$ for $d_b \to \infty$, this explicitly shows that the coherence of this first excitation is vanishing. At the same time, it demonstrates that the photon scattering from its local density preserves the coherence of all other excitations, since $\Phi_1(x_{\min}, y_{\min} = x_{\min}) = 1$.

As described above, the efficiency of gate photon retrieval is directly affected by scattering induced spin wave decoherence. While this inhibits the retrieval of a single gate excitation [46], the many-body decoherence protection between multiple gate excitations offers enhanced retrieval efficiencies, relative to the case of a single excitation. Here we derive a simplified description of gate photon retrieval from the full many-body density matrix $\rho_{n_s}(\vec{x}_{n_g}, \vec{y}_{n_g})$ in Eq. (2), by assuming that scattering off one gate excitation leaves the mode shape, and thus retrieval efficiency, of all other excitations unaffected.

Considering coherent gate and source fields containing an average number of photons α_g and α_s, respectively, we calculate the retrieval efficiency of each gate excitation sequentially from its reduced density matrix. The total retrieval efficiency η can then be written as [51]

$$\eta = \eta_R \frac{e^{-\alpha_g}}{\alpha_g} \sum_{n_g=1}^{\infty} \frac{(\alpha_g)^{n_g}}{n_g!} \sum_{k=1}^{n_g} e^{-\alpha_s p(1-p)^{(k-1)}}, \qquad (5)$$

where $p \approx 1 - \exp[-4d_b]$ is the source photon scattering probability per gate excitation, and η_R denotes the retrieval efficiency in the absence of interactions between source and gate excitations. The second summand in Eq. (5) is proportional to the probability of retrieving the kth excitation in a given Fock state component of the stored field. From this it is clear that in the strong scattering limit ($p \sim 1$), the retrieval of the first excitation ($k = 1$) is suppressed, while the retrieval of all later excitations ($k > 1$) is largely unaffected. The retrieval efficiency thus provides a well suited and accessible experimental probe of the many-body decoherence in the system.

Our experiments start by trapping $\sim 9 \times 10^4$ ^{87}Rb atoms into an optical dipole trap which yields a cigar-shaped cloud at 4 μK with $1/e$ radial and axial radii of 13 and 42 μm, respectively. All atoms are first optically pumped into the $|g\rangle = |5S_{1/2}, F = 2, m_F = 2\rangle$ state. Gate photons are coupled to the Rydberg state $|c\rangle = |68S_{1/2}, m_J = 1/2\rangle$ via EIT by applying a weak 780 nm probe field that drives the transition between $|g\rangle$ and the intermediate $|p\rangle = |5P_{3/2}, F = 3, m_F = 3\rangle$ state. A strong counterpropagating 480 nm control field drives the transition between $|p\rangle$ and $|c\rangle$ with a Rabi frequency Ω_g on two-photon resonance to establish EIT. We store gate photons in the cloud by turning off Ω_g while the gate photon pulse propagates through the cloud. The generated number of Rydberg excitations can be measured by standard field ionization detection from which we determine α_g. Using a source photon pulse with an average number of α_s photons, we can probe the stored gate excitations optically by monitoring the source-photon transmission. In this case, EIT is provided by another control laser that couples the intermediate state to the $|s\rangle = |66S_{1/2}, m_J = 1/2\rangle$ Rydberg state. Following their interaction with the source photons, the gate photons are read out by turning Ω_g back on after a total storage time of 4 μs. A typical complete pulse sequence is shown in Fig. 1(c).

In Fig. 2 we show the retrieval efficiency as a function of the number $\bar{\alpha}_s$ of gate-scattered source photons, which we determine from the transmission in the absence and presence of the gate excitations. If the photon-photon interactions would decohere all gate excitations, the retrieval efficiency would scale as $\eta_R \exp[-\bar{\alpha}_s/\alpha_g]$, which simply reflects the vacuum component of the source-photon pulse [46]. While this simple relation yields a good description for small α_g and $\bar{\alpha}_s$, we observe significantly higher retrieval efficiencies for larger photon numbers.
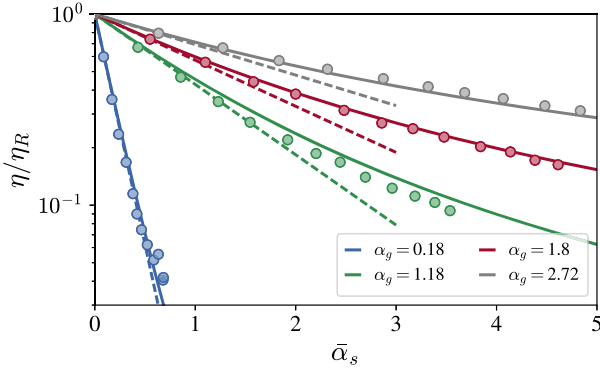
FIG. 2. Normalized retrieval efficiency as a function of the number $\bar{\alpha}_s$ of scattered source photons for different indicated numbers α_g of stored gate excitations. The theoretical prediction of Eq. (5) (solid lines) is fitted to the experimental data (dots) with a common scattering probability of $p = 0.5$ (errors bars showing SEM are smaller than the dots). Retrieval efficiencies are on the order of $\eta_R \sim 0.2$ for all measured data. The dashed lines indicate the expected scaling without decoherence protection.
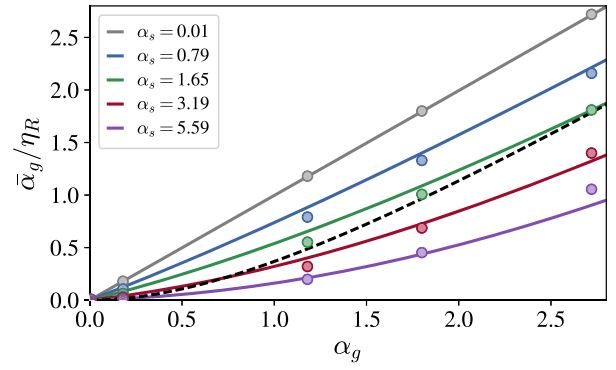

FIG. 3. Number $\bar{\alpha}_g$ of retrieved gate photons as a function of the number α_g of initially stored excitations for different incident source photon numbers α_s. The measurements (dots) agree well with the prediction of Eq. (5) (solid lines) for the same value of p as in Fig. 2. The black dashed line shows the prediction of Eq. (5) for $p = 1$ and large source field intensity $\alpha_s \gg 1$, which are the ideal conditions for single-photon subtraction.

Indeed, this can be traced back to the multiphoton protection mechanism introduced in this work, as further evidenced by the remarkably good agreement with the theoretical prediction of Eq. (5).

As the scattering probability approaches unity, only the first gate excitation participates in the decoherence dynamics. This in turn enables a robust mechanism for single-photon subtraction, since the inability to retrieve the decohered excitation effectively removes a single photon from the initial gate field upon retrieval. Figure 3 shows the number $\bar{\alpha}_g$ of retrieved gate photons as a function of the number of stored gate excitations. Note that the number of subtracted photons can still exceed unity due to the imperfect scattering conditions, $p < 1$, in the experiment. In this case, the first gate excitation does not completely extinguish the source field which can, therefore, decohere additional gate photons. For the source field intensities considered in Fig. 3, the measured transmitted intensity is linear, indicating that self-interactions between source photons have a negligible effect.

To analyze the optimal operation of the photon subtractor, we define the probability $\mathcal{F}$ that exactly one photon is decohered by source photon scattering. Using the theory outlined above, we obtain [51]

$$\mathcal{F} = e^{-\alpha_g} \left[1 + \sum_{n_g=1}^{\infty} \frac{(\alpha_g)^{n_g}}{n_g!} P_1(n_g, \alpha_s) \right], \qquad (6)$$

where $P_1(n_g, \alpha_s)$ is the probability that the source field decoheres exactly one of the n_g stored excitations in a given stored Fock state component. Upon maximizing Eq. (6) with respect to α_s we obtain the optimal subtraction efficiency $\mathcal{F}_{\text{opt}}$. We plot $\mathcal{F}_{\text{opt}}$ in Fig. 4, and compare this to the corresponding performance of an alternative subtraction

mechanism recently demonstrated in Ref. [54]. Such alternative schemes utilize quantum emitters whose absorption can be saturated by a single photon, e.g., through strong photon coupling to a single atom [16] or by exploiting the Rydberg blockade in atomic ensembles [54,55].

To draw this comparison, we have calculated the optimal subtraction efficiency of the approach demonstrated in Ref. [54]. The details of this calculation are outlined in Ref. [51]. Here one employs Rydberg state dephasing with a rate Γ for efficient single-photon absorption with probability p. Working with a small ensemble, the produced Rydberg excitation then blocks the storage of subsequent photons and renders the medium largely transparent with a small residual absorption. While this strategy benefits from the growing single-photon absorption efficiency with
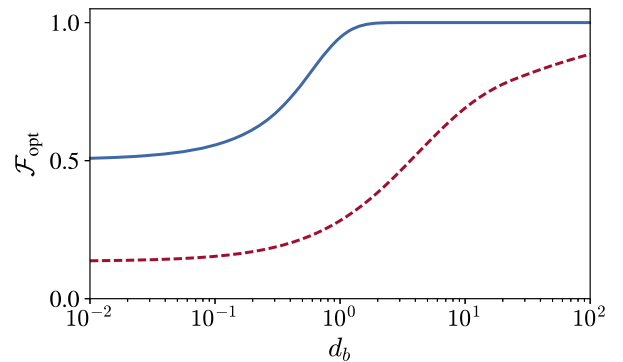

FIG. 4. Single-photon subtraction efficiency, $\mathcal{F}_{\text{opt}}$, for a coherent gate field with an average number of photons $\alpha_g = 2$. The blue line shows the optimal efficiency of the current mechanism based on single-photon decoherence for perfect storage and retrieval, while the red dashed line shows the corresponding performance of photon subtraction by saturable absorption [54].

increasing input power [54], its fidelity is ultimately limited by the challenging requirement of maximizing p at low residual photon absorption. In the present case, the scattering probability p exponentially approaches unity with increasing d_b, which simultaneously enhances the protection of all other photons from decoherence, and thereby improves the overall subtractor performance. Instead, the overall performance is limited by the finite storage and retrieval efficiency [51]. While the current experiment has not been optimized with respect to storage and retrieval, we note that recent measurements have reported combined efficiencies in excess of 95% [56]. Approaching this limit in Rydberg media would require longer clouds with higher optical depth and shorter storage times to minimize dephasing effects [57], combined with optimization of the storage and retrieval protocol [46–48].

In summary, we have investigated the dissipative quantum dynamics of multiple photons in a strongly interacting Rydberg ensemble. Considering the specific situation of stored Rydberg spin waves interacting with propagating Rydberg polaritons, we derived an exact solution to this general many-body problem, which reveals correlated spin wave dynamics and a mutual decoherence protection mechanism between multiple stored excitations. Our experiments clearly demonstrate this effect and suggest how it can be exploited to manipulating light at the quantum level. In particular, we showed how the discovered effect can provide a robust mechanism for realizing a single-photon subtractor. Its current overall performance is limited by the efficiency for light storage and retrieval. Improving this capability and better understanding associated Rydberg-state effects [44,58–61] will thus be central to future work, and is vital to a number of recent experiments [38–42,44,62] based on light storage and subsequent photon interactions. Our measurements and developed theory of multiphoton decoherence effects provide valuable insights for such applications [38–42] and future studies of strongly interacting Rydberg-polariton systems beyond the few photon limit.

[1] S. Diehl, A. Micheli, A. Kantian, B. Kraus, H. P. Büchler, and P. Zoller, Nat. Phys. **4**, 878 (2008).

[2] F. Verstraete, M. M. Wolf, and J. Ignacio Cirac, Nat. Phys. **5**, 633 (2009).

[3] J. T. Barreiro, M. Muller, P. Schindler, D. Nigg, T. Monz, M. Chwalla, M. Hennrich, C. F. Roos, P. Zoller, and R. Blatt, Nature (London) **470**, 486 (2011).

[4] S. Diehl, E. Rico, M. A. Baranov, and P. Zoller, Nat. Phys. **7**, 971 (2011).

[5] F. Reiter, D. Reeb, and A. S. Sørensen, Phys. Rev. Lett. **117**, 040501 (2016).

[6] T. Ramos, H. Pichler, A. J. Daley, and P. Zoller, Phys. Rev. Lett. **113**, 237203 (2014).

[7] H. Pichler, T. Ramos, A. J. Daley, and P. Zoller, Phys. Rev. A **91**, 042116 (2015).

[8] D. E. Chang, V. Vuletić, and M. D. Lukin, Nat. Photonics **8**, 685 (2014).

[9] K. M. Birnbaum, A. Boca, R. Miller, A. D. Boozer, T. E. Northup, and H. J. Kimble, Nature (London) **436**, 87 (2005).

[10] J. Hwang, M. Pototschnig, R. Lettow, G. Zumofen, A. Renn, S. Götzinger, and V. Sandoghdar, Nature (London) **460**, 76 (2009).

[11] S. Faez, P. Türschmann, H. R. Haakh, S. Götzinger, and V. Sandoghdar, Phys. Rev. Lett. **113**, 213601 (2014).

[12] A. Maser, B. Gmeiner, T. Utikal, S. Götzinger, and V. Sandoghdar, Nat. Photonics **10**, 450 (2016).

[13] D. O'Shea, C. Junge, J. Volz, and A. Rauschenbeutel, Phys. Rev. Lett. **111**, 193601 (2013).

[14] J. Volz, M. Scheucher, C. Junge, and A. Rauschenbeutel, Nat. Photonics **8**, 965 (2014).

[15] I. Shomroni, S. Rosenblum, Y. Lovsky, O. Bechler, G. Guendelman, and B. Dayan, Science **345**, 903 (2014).

[16] S. Rosenblum, O. Bechler, I. Shomroni, Y. Lovsky, G. Guendelman, and B. Dayan, Nat. Photonics **10**, 19 (2016).

[17] T. G. Tiecke, J. D. Thompson, N. P. de Leon, L. R. Liu, V. Vuletić, and M. D. Lukin, Nature (London) **508**, 241 (2014).

[18] A. Javadi, I. Söllner, M. Arcari, S. L. Hansen, L. Midolo, S. Mahmoodian, G. Kiršansk, T. Pregnolato, E. H. Lee, J. D. Song, S. Stobbe, and P. Lodahl, Nat. Commun. **6**, 8655 (2015).

[19] A. Reiserer, S. Ritter, and G. Rempe, Science **342**, 1349 (2013).

[20] A. Reiserer, N. Kalb, G. Rempe, and S. Ritter, Nature (London) **508**, 237 (2014).

[21] J. S. Douglas, T. Caneva, and D. E. Chang, Phys. Rev. X **6**, 031017 (2016).

[22] T. Peyronel, O. Firstenberg, Q.-Y. Liang, S. Hofferberth, A. V. Gorshkov, T. Pohl, M. D. Lukin, and V. Vuletić, Nature (London) **488**, 57 (2012).

[23] O. Firstenberg, T. Peyronel, Q.-Y. Liang, A. V. Gorshkov, M. D. Lukin, and V. Vuletić, Nature (London) **502**, 71 (2013).

[24] J. D. Thompson, T. L. Nicholson, Q.-Y. Liang, S. H. Cantu, A. V. Venkatramani, S. Choi, I. A. Fedorov, D. Viscor, T. Pohl, M. D. Lukin, and V. Vuletić, Nature (London) **542**, 206 (2017).

[25] I. Carusotto, D. Gerace, H. E. Tureci, S. De Liberato, C. Ciuti, and A. Imamoglu, Phys. Rev. Lett. **103**, 033601 (2009).

[26] F. Nissen, S. Schmidt, M. Biondi, G. Blatter, H. E. Türeci, and J. Keeling, Phys. Rev. Lett. **108**, 233603 (2012).

[27] M. Hafezi, M. D. Lukin, and J. M. Taylor, New J. Phys. **15**, 063001 (2013).

[28] M. F. Maghrebi, N. Y. Yao, M. Hafezi, T. Pohl, O. Firstenberg, and A. V. Gorshkov, Phys. Rev. A **91**, 033838 (2015).

[29] E. Zeuthen, M. J. Gullans, M. F. Maghrebi, and A. V. Gorshkov, Phys. Rev. Lett. **119**, 043602 (2017).

[30] M. Fleischhauer, A. Imamoglu, and J. P. Marangos, Rev. Mod. Phys. **77**, 633 (2005).

[31] M. Saffman, T. G. Walker, and K. Mølmer, Rev. Mod. Phys. **82**, 2313 (2010).

[32] I. Friedler, D. Petrosyan, M. Fleischhauer, and G. Kurizki, Phys. Rev. A **72**, 043803 (2005).

[33] D. Petrosyan, J. Otterbach, and M. Fleischhauer, Phys. Rev. Lett. **107**, 213601 (2011).

[34] C. Murray and T. Pohl, *Advances In Atomic, Molecular, and Optical Physics* (Academic Press, New York, 2016), Vol. 65, p. 321.

[35] O. Firstenberg, C. S. Adams, and S. Hofferberth, J. Phys. B **49**, 152003 (2016).

[36] M. D. Lukin, M. Fleischhauer, R. Cote, L. M. Duan, D. Jaksch, J. I. Cirac, and P. Zoller, Phys. Rev. Lett. **87**, 037901 (2001).

[37] J. D. Pritchard, D. Maxwell, A. Gauguet, K. J. Weatherill, M. P. A. Jones, and C. S. Adams, Phys. Rev. Lett. **105**, 193603 (2010).

[38] S. Baur, D. Tiarks, G. Rempe, and S. Dürr, Phys. Rev. Lett. **112**, 073901 (2014).

[39] D. Tiarks, S. Baur, K. Schneider, S. Dürr, and G. Rempe, Phys. Rev. Lett. **113**, 053602 (2014).

[40] H. Gorniaczyk, C. Tresp, J. Schmidt, H. Fedder, and S. Hofferberth, Phys. Rev. Lett. **113**, 053601 (2014).

[41] H. Gorniaczyk, C. Tresp, P. Bienias, A. Paris-Mandoki, W. Li, I. Mirgorodskiy, H. P. Büchler, I. Lesanovsky, and S. Hofferberth, Nat. Commun. **7**, 12480 (2016).

[42] D. Tiarks, S. Schmidt, G. Rempe, and S. Dürr, Sci. Adv. **2**, e1600036 (2016).

[43] M. J. Gullans, S. Diehl, S. T. Rittenhouse, B. P. Ruzic, J. P. D'Incao, P. Julienne, A. V. Gorshkov, and J. M. Taylor, Phys. Rev. Lett. **119**, 233601 (2017).

[44] Q.-Y. Liang, A. V. Venkatramani, S. H. Cantu, T. L. Nicholson, M. J. Gullans, A. V. Gorshkov, J. D. Thompson, C. Chin, M. D. Lukin, and V. Vuletic, Science **359**, 783 (2018).

[45] W. Li and I. Lesanovsky, Phys. Rev. A **92**, 043828 (2015).

[46] C. R. Murray, A. V. Gorshkov, and T. Pohl, New J. Phys. **18**, 092001 (2016).

[47] A. V. Gorshkov, A. André, M. Fleischhauer, A. S. Sørensen, and M. D. Lukin, Phys. Rev. Lett. **98**, 123601 (2007).

[48] A. V. Gorshkov, A. André, M. D. Lukin, and A. S. Sørensen, Phys. Rev. A **76**, 033805 (2007).

[49] I. Novikova, A. V. Gorshkov, D. F. Phillips, A. S. Sørensen, M. D. Lukin, and R. L. Walsworth, Phys. Rev. Lett. **98**, 243602 (2007).

[50] A. V. Gorshkov, J. Otterbach, M. Fleischhauer, T. Pohl, and M. D. Lukin, Phys. Rev. Lett. **107**, 133602 (2011).

[51] See Supplemental Material at http://link.aps.org/supplemental/10.1103/PhysRevLett.120.113601 for details on the calculation of the many-body density matrix dynamics, gate photon retrieval efficiency, and single photon subtraction efficiencies, which includes Refs. [52,53].

[52] M. O. Scully and M. S. Zubairy, *Quantum Optics* (Cambridge University Press, Cambridge, England, 1997).

[53] A. V. Gorshkov, R. Nath, and T. Pohl, Phys. Rev. Lett. **110**, 153601 (2013).

[54] C. Tresp, C. Zimmer, I. Mirgorodskiy, H. Gorniaczyk, A. Paris-Mandoki, and S. Hofferberth, Phys. Rev. Lett. **117**, 223001 (2016).

[55] J. Honer, R. Löw, H. Weimer, T. Pfau, and H. P. Büchler, Phys. Rev. Lett. **107**, 093601 (2011).

[56] Y.-F. Hsiao, P.-J. Tsai, H.-S. Chen, S.-X. Lin, C.-C. Hung, C.-H. Lee, Y.-H. Chen, Y.-F. Chen, I. A. Yu, and Y.-C. Chen, arXiv:1605.08519.

[57] I. Mirgorodskiy, F. Christaller, C. Braun, A. Paris-Mandoki, C. Tresp, and S. Hofferberth, Phys. Rev. A **96**, 011402 (2017).

[58] A. Gaj, A. T. Krupp, J. B. Balewski, R. Löw, S. Hofferberth, and T. Pfau, Nat. Commun. **5**, 4546 (2014).

[59] R. Schmidt, H. R. Sadeghpour, and E. Demler, Phys. Rev. Lett. **116**, 105302 (2016).

[60] F. Camargo, R. Schmidt, J. D. Whalen, R. Ding, G. Woehl, S. Yoshida, J. Burgdörfer, F. B. Dunning, H. R. Sadeghpour, E. Demler, and T. C. Killian, Phys. Rev. Lett. **120**, 083401 (2018).

[61] R. Schmidt, J. D. Whalen, R. Ding, F. Camargo, G. Woehl, S. Yoshida, J. Burgdorfer, F. B. Dunning, E. Demler, H. R. Sadeghepour, and T. C. Killian, Phys. Rev. A **97**, 022707 (2018).

[62] H. Busche, P. Huillery, S. W. Ball, T. Ilieva, M. P. A. Jones, and C. Adams, Nat. Phys. **13**, 655 (2017).